Synthesis of ZnO nanocrystals by subsequent implantation of Zn and O species

J. K. Lee,[a] C. R. Tewell, R. K. Schulze, and M. Nastasi
Materials Science and Technology Division, Los Alamos National Laboratory, New Mexico 87544

D. W. Hamby and D. A. Lucca
School of Mechanical and Aerospace Engineering, Oklahoma State University, Oklahoma 74078

H. S. Jung and K. S. Hong
Materials Science and Engineering, Seoul National University, Seoul 151-742, Korea

(Received 7 September 2004; accepted 9 March 2005; published online 29 April 2005)

We report the preparation of ZnO nanocrystals embedded in a SiO_2 matrix formed using sequential zinc and oxygen ion implantations. The optical absorption spectra and photoemission spectra of zinc implanted and zinc/oxygen coimplanted silica show that the first zinc implantation produces zinc clusters and that the subsequent oxygen implantation following the zinc implantation rearranges the distribution of zinc and oxygen ions at an atomic level. While thermal annealing of Zn only implanted silica leads to the formation of Zn nanocrystals, thermal annealing of zinc/oxygen coimplanted silica promotes the growth of ZnO nanocrystals. The absorption and photoluminescence spectra show that ZnO nanocrystals form in an amorphous SiO_2 matrix and that their systematic change as a function of annealing temperature corresponds to the typical correlation between the increase of particle size and a redshift in near-band-edge emission.
 [DOI: 10.1063/1.1906304]

Following the demonstration of blue-green light-emitting diodes (LEDs) and lasers using II–VI compounds, there has been intensive investigation of wide-band-gap II–VI compounds for optoelectric applications in both the visible and ultraviolet (UV) regions. Among several wide-band-gap II–VI semiconductor materials of interest, ZnO has attracted tremendous attention due to its high exciton binding energy (60 meV),[1,2] as compared to 25 meV for GaN, and 20 meV for ZnSe. This large exciton binding energy of ZnO allows excitonic recombination and optically pumped laser oscillations even at room temperature.[3]

Semiconductor nanocrystals, having dimensions comparable to the Bohr exciton diameter, exhibit changes in optical luminescence spectra due to quantum confinement of excitons and the dielectric functional confinement.[4–6] The unique properties of semiconducting nanocrystals have motivated a number of studies on ZnO nanocrystals, which were manufactured using various synthesis methods.[7–9] However, one of the central problems of ZnO nanocrystals is that the desired UV band-gap luminescence is weak.[10–13]

One solution for enhancing the near-band-edge emission UV emission in ZnO nanocrystals is to encapsulate the nanocrystals with protective surface layers.[14] Ion implantation is an effective method to synthesize matrix embedded nanocrystals with controlled particle size, crystallographic orientation, lattice structure, and spatial density.[15,16] In the present study, ion implantation was utilized to produce ZnO nanocrystals buried in a dielectric host material (amorphous SiO_2). Using sequential ion implantation of Zn and O, encapsulated ZnO nanocrystals were successfully prepared. These nanocrystals, with sizes comparable to the Bohr exciton diameter (3 nm),[17] exhibited a strong UV emission at room temperature and a behavior consistent with the quantum confinement effect.

Optical grade amorphous silica (α-SiO_2) substrates were implanted with 100 keV Zn^+ at doses of 1, 3, 5, and 10×10^{16} ions/cm^2. Subsequently, O^+ ions were implanted with an energy of 57 keV at doses of 1, 3, 5, and 10×10^{16} ions/cm^2 into the same range as the Zn^+ ions in half of the Zn preimplanted substrates. All implantations were performed at room temperature. These two sets of samples (Zn only implanted substrates and Zn+O sequentially implanted substrates) were annealed in either a vacuum or oxygen atmosphere at several temperatures ranging from 300 to 700 °C.

The concentration profiles of implanted ions were measured before and after the thermal treatment by Rutherford backscattering spectroscopy (RBS). Optical absorption measurements of implanted silica were performed with a Cary 5E spectrophotometer at room temperature. The chemical state of Zn in the silica matrix was analyzed with the aid of x-ray photoemission spectroscopy (XPS) to verify the creation of ZnO particles using a PHI5600 ESCA System. The C 1*s* and Si 2*p* peaks were used to calibrate the binding energy of spectra. During XPS measurement, sputtering was performed to investigate the depth profiles of samples. The PL spectra of nanocrystals were measured by using the 266 nm line from a Nd-YAG laser and photomultiplier detector.

Figure 1 shows the optical absorption curves for as-implanted and annealed silica with Zn doses of 1, 3, 5, and 10×10^{16} ions/cm^2. With increasing Zn ion dose, the background of the spectra increased and the absorption spectra exhibited a peak. For the sample implanted with 10×10^{16} Zn/cm^2, an absorption peak was observed at 255 nm. As the annealing temperature of the as-implanted samples was increased, the absorption peak of the Zn implanted

[a]Author to whom correspondence should be addressed; electronic mail: jklee@lanl.gov

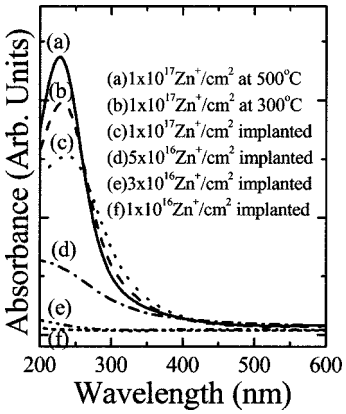

FIG. 1. Optical absorbance curves for Zn ion as-implanted and annealed silica substrates with different doses: $1\times10^{16}/\mathrm{cm}^2$, $5\times10^{16}/\mathrm{cm}^2$, $1\times10^{17}/\mathrm{cm}^2$.

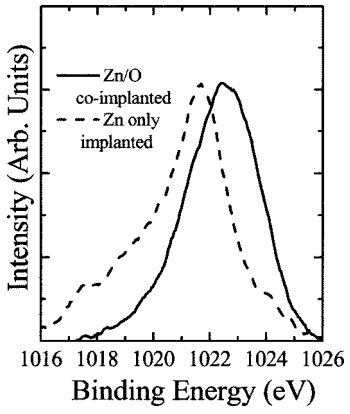

FIG. 3. Zn $3p$ core levels of x-ray photoemission spectra (XPS) data of for Zn implanted or Zn/O coimplanted and annealed silica with a dose of $1\times10^{17}/\mathrm{cm}^2$ at a depth of Zn concentration peak.

samples exhibited a progressive blueshift in peak position and a decrease in peak width. Also, the annealing process decreased the background spectra above 300 nm, which increased during the Zn implantation process.

The optical absorption spectra for sequentially implanted and annealed silica with a Zn dose of 1×10^{17} ions/cm^2 and O ion dose of 1×10^{17} ions/cm^2 are shown in Fig. 2. In contrast to the Zn only implantation, the sequential implantation of Zn and O resulted in the reduction of the 255 nm absorption peak and the appearance of a new band around 290 nm. While the absorption peak at 255 nm observed in the Zn only implanted silica showed a blueshift with increasing annealing temperature, the new band at 290 nm observed in sequentially implanted samples showed a redshift with increasing annealing temperature.

Photoemission spectra of Zn $3p$ for Zn only implanted/annealed and Zn/O sequentially implanted/annealed silica are shown in Fig. 3. In Zn only implanted silica, the binding energy of the Zn $3p$ peak, at the depth of maximum Zn concentration (40 nm), was 1021 eV, the binding energy of metallic Zn, which reveals the formation of metallic Zn clusters after Zn only implantation and subsequent annealing.[18] However, when Zn and O were coimplanted and annealed, the binding energy of the Zn $3p$ peak was found to be 1023 eV, close to the binding energy of ZnO. This shift of the binding energy of the Zn $3p$ peak toward a higher value in Zn and O coimplanted silica indicates that the coimplanted O ions promoted the formation of ZnO crystals.

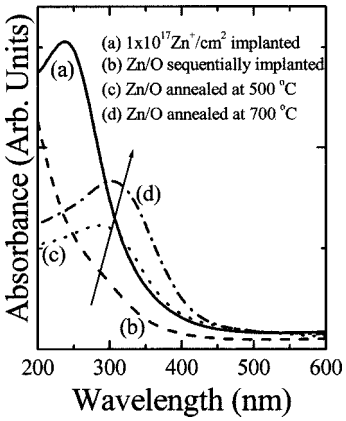

FIG. 2. Optical absorbance curves for Zn and O sequentially implanted and annealed silica.

It is well known that the ion-irradiation damage that occurs in ion implanted silica creates defects and causes changes in its optical response.[19] However, the peaks of the optical absorption curve of Zn only implanted silica in the range of 210–260 nm cannot be fully explained by defect generation, for the subsequent O implantation removed the peaks observed in the absorption curves of Zn only implanted silica despite the further increase in irradiation damage caused by the second implantation. The increase in the intensity and sharpness of optical absorption peak after thermal annealing also indicates that the peak near 255 nm does not result from the irradiation damage, for thermal annealing promotes recovery of irradiation damage and decreases the absorption due to defects.

According to Chen *et al.*, surface plasmon absorption was observed at 240 nm for Zn clusters,[20] which suggests that high-dose Zn implantation and subsequent annealing in this study formed Zn clusters instead of ZnO nanocrystals. The size of the Zn clusters from Zn only implantation was calculated using Mie scattering theory and the width of the absorption peaks. Using a refractive index of 1.5 and a dielectric constant of 4.9 for glass, Zn clusters were found to be 2.0 nm when Zn only implanted samples were annealed at 500 °C.[21,22] The redshift of the absorption peak position with annealing, can be explained by the overflow of conduction electrons from metal nanocrystals smaller than 10 nm.[23]

After the subsequent O implantation into Zn preimplanted silica, the absorption peak observed at 250 nm, which is attributed to Zn clusters, disappears. This disappearance of an absorption peak warrants a detailed examination on the kinetics of nanocrystal growth during the sequential Zn and O implantation process. When metal clusters in the preimplanted layer are subsequently irradiated with different ions, the preexisting clusters are broken down and the second irradiation promotes the nucleation of new precipitates around the periphery of the preexisting clusters, which is called inverse Ostwald ripening.[24,25] The literature on inverse Ostwald ripening suggests that the subsequent O implantation decomposed the preexisting Zn clusters, allowing for the nucleation of new ZnO nanocrystals. The optical absorption spectra observed for coimplanted samples are consistent with this suggestion that the subsequent O implantation destroyed the preexisting Zn clusters thus enhancing the formation of ZnO nanocrystals. While the optical absorption peak at 255 nm was observed for Zn only implanted samples, the Zn and O coimplanted and annealed silica exhibited an absorp-

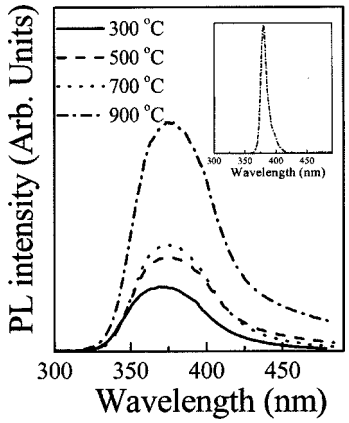

FIG. 4. Room temperature, steady state photoluminescence for Zn and O coimplanted silica samples with a dose of $1\times10^{17}/\mathrm{cm}^2$ which were annealed at 300, 500, 700, and 900 °C. (PL spectra of ZnO single crystal is shown as an inset.)

tion peak between 300 and 350 nm where the absorption of ZnO was observed. The presence of ZnO nanocrystals is also supported by the photoemission spectra shown in Fig. 3. It shows a shift in the binding energy of the Zn 3*p* peak from the indicative of pure Zn (1021 eV) to that of ZnO (1023 eV). The shift in the binding energy demonstrates that Zn in only Zn implanted silica remains metallic zinc while Zn/O coimplantation produces the ZnO phase.

Moreover, the photoluminescence (PL) spectra of coimplanted samples shown in Fig. 4 support our assertion that the subsequent oxygen implantation reconstructed Zn clusters, leading to the formation of ZnO nanocrystals. While the PL spectrum of Zn only implanted silica did not show any PL peaks in the measured range, the PL spectra of annealed samples demonstrate the formation of ZnO. Each annealed sample exhibits a RT PL peak around 370 nm, which is consistent with the RT band gap of ZnO.[26] The intensity of this peak is observed to grow with increasing annealing temperature. This strong UV emission shows that the coimplantation of Zn and O ions in this study can result in near-band-edge emission luminescence which is stronger than the surface defect-related green emission by a factor of 5, contrary to previous observations for ZnO nanocrystals.[10,11] This enhanced near-band-edge emission of sequentially implanted silica compared with green emission is attributed to the effective encapsulation and passivation of the ZnO nanocrystals surface by the silica matrix. Figure 4 also shows that there is a small redshift of the PL peak position from 365 to 375 nm with increased annealing temperature. This shift could be attributed to the near-band-edge emission of strongly confined nanocrystals whose diameter is comparable to the Bohr diameter. If it is the result of quantum confinement,[27,28] the size of ZnO nanocrystal is calculated to be between 2.2 and 3.0 nm, following the effective mass model for the energy gap.[29] However, it should be noted that the strain effect and Stoke's shift could also contribute to the change in PL spectra. Residual strain in ZnO nanocrystals from thermal stress and ion implantation is known to induce a complicated behavior in the luminescence of ZnO nanocrystals.[30] The Stokes' shift, defined as the energy difference between energy band gap and the peak of the emission spectrum also indicates that the localized states of excitons affected PL spectra of ZnO nanocrystals, which was more pronounced in low temperature annealed nanocrystals.[31] More investigation is in progress to find the correlation between nanocrystal size and luminescence properties using transmissional electron microscopy and low temperature PL.

This work has been supported by the U.S. Department of Energy Office of Basic Energy Sciences. The authors wish to thank the technical staff of the Los Alamos Ion Beam Materials Laboratory for their assistance in performing this research.

[1] E. Mollwo, in *Semiconductors: Physics of II-VI and I-VII Compounds, Semimagnetic Semiconductors, Landolt-Börnstein New Series*, edited by O. Madelung, M. Schulz, and H. Weiss (Springer, Berlin, 1982), Vol. 17, p. 35.
[2] K. Hümmer, Phys. Status Solidi B **56**, 249 (1973).
[3] D. M. Bagnall, Y. F. Chen, Z. Zhu, T. Yao, S. Koyama, M. Y. Shen, and T. Goto, Appl. Phys. Lett. **70**, 2230 (1997).
[4] C. Weisbuch and B. Vinter, in *Quantum Semiconductor Structures* (Academic, San Diego, 1991).
[5] S. V. Gaponenko, in *Optical Properties of Semiconductor Nanocrystals* (Cambridge University Press, Cambridge, 1998).
[6] P. Chakraborty, J. Mater. Sci. **33**, 2235 (1998).
[7] U. Koch, A. Fojtik, H. Weller, and A. Henglein, Chem. Phys. Lett. **122**, 507 (1985).
[8] S. Sakohara, M. Ishida, and M. A. Anderson, J. Phys. Chem. B **102**, 10169 (1998).
[9] E. M. Wong, J. E. Bonevich, and P. C. Searson, J. Phys. Chem. B **102**, 7770 (1998).
[10] A. V. Dijken, D. A. Meukenkamp, D. Vanmaekelbergh, and A. Meijerink, J. Lumin. **87**, 454 (2000).
[11] L. Spanhel and M. A. Anderson, J. Am. Chem. Soc. **113**, 2826 (1991).
[12] K. Borgohain and S. Mahamuni, Semicond. Sci. Technol. **13**, 1154 (1998).
[13] H. Zhou, H. Alves, D. M. Hofmann, W. Kriegseis, B. K. Meyer, G. Kaczmarczyk, and A. Hoffman, Appl. Phys. Lett. **80**, 210 (2002).
[14] L. Guo, S. Yang, C. Yang, P. Yu, J. Wang, W. Ge, and G. K. L. Wong, Appl. Phys. Lett. **76**, 2901 (2000).
[15] J. D. Budai, C. W. White, S. P. Withrow, M. F. Chisholm, J. Zhu, and R. A. Zuhr, Nature (London) **390**, 384 (1997).
[16] A. Meldrum, L. A. Boatner, and C. W. White, Nucl. Instrum. Methods Phys. Res. B **178**, 7 (2001).
[17] S. B. Orlinskii, J. Schmidt, P. G. Baranov, D. M. Hofmann, C. D. Donega, and A. Meijerink, Phys. Rev. Lett. **92**, 047603 (2004).
[18] J. F. Moulder, W. F. Stickle, P. E. Sobol, and K. D. Bomben, in *Handbook of X-Ray Photoelectron Spectroscopy*, edited by J. Chastain and R. C. King (Physical Electronics, Eden Prairie, MN, 1992).
[19] G. W. Arnold, J. Non-Cryst. Solids **179**, 288 (1994).
[20] J. Chen, R. Mu, A. Ueda, M. H. Wu, Y.-S. Tung, Z. Gu, D. O. Henderson, C. W. White, J. D. Budai, and R. A. Zuhr, J. Vac. Sci. Technol. A **16**, 1409 (1998).
[21] G. Mie, Ann. Phys. **25**, 377 (1908).
[22] W. J. Doyle, Phys. Rev. **111**, 1067 (1958).
[23] U. Kreibig and M. Vollmer, in *Optical Properties of Metal Clusters* (Springer, New York, 1995), p. 118.
[24] M. Strobel, K.-H. Heinig, and W. Möller, Phys. Rev. B **64**, 024522 (2001).
[25] G. C. Rizza, M. Strobel, K.-H. Heinig, and H. Bernas, Nucl. Instrum. Methods Phys. Res. B **178**, 78 (2001).
[26] Y. Chen, D. M. Bagnall, H. J. Koh, K. T. Park, K. Hiraga, Z. Zhu, and T. Yao, J. Appl. Phys. **84**, 3912 (1998).
[27] S. Cho, J. Ma, Y. Kim, Y. Sun, G. K. L. Wong, and J. B. Ketterson, Appl. Phys. Lett. **75**, 2761 (1999).
[28] E. M. Wong and P. C. Searson, Appl. Phys. Lett. **74**, 2939 (1999).
[29] L. E. Brus, J. Chem. Phys. **80**, 4403 (1984).
[30] E. S. Kim, N. Usami, and Y. Shiraki, Appl. Phys. Lett. **70**, 297 (1997).
[31] K. P. O'Donnell, R. W. Martin, and P. G. Middleton, Phys. Rev. Lett. **82**, 237 (1999).